# Genes, mechanisms and novel EST-SSR markers associated with metribuzin tolerance in wheat (*Triticum aestivum L.*): targets for improving photosynthetic capacity and yield

**Roopali Bhoite**
University of Western Australia Faculty of Science
**Ping Si**
University of Western Australia Faculty of Science
**Kadambot H. M. Siddique**
University of Western Australia Faculty of Science
**Guijun Yan** ( guijun.yan@uwa.edu.au )
University of Western Australia Faculty of Science https://orcid.org/0000-0001-9628-1211

**Research article**

**Keywords:** Metribuzin tolerant genes, ROS detoxification pathways, ROS homeostasis, Transcription factors, Phytohormones, Gene-based EST-SSR markers, Light-harvesting chlorophyll (Lhc) a/b-binding proteins, PSII stability factor HCF136

**Posted Date:** June 4th, 2020

**DOI:** https://doi.org/10.21203/rs.3.rs-29235/v1

## Abstract

# Background

Weed infestation is one of the major yield-reducing factors in wheat in dry-land farming. Metribuzin is a broad-spectrum herbicide which allow effective weed management in wheat but the narrow safety margin results in crop damage decreasing grain yield. Improving our understanding of the genetic and genomic basis for metribuzin tolerance opens the potential to enhance herbicide tolerance and better productivity in wheat. The present investigation examines the genes involved in regulation of metribuzin tolerance including genetic/signalling pathways, transcription factors, phytohormones, and gene based EST-SSR markers related to photosynthesis and metabolic detoxification.

# Results

Transcriptome sequencing of most diverse genotypes using high throughput NovaSeq 6000 RNA-Seq platform identified a total of 77,443 genes, of which 59,915 were known genes and 17,528 were novel genes. The integrative analyses of the expression profiles of genes and pathways at 0 h, 24 h and 60 h herbicide exposure indicated that modulation of reactive oxygen species (ROS) homeostasis and endogenous increase of light-harvesting chlorophyll (*Lhc)* a/b-binding proteins, PSII stability factor HCF136, metabolic detoxification enzymes (peroxidase, cytochrome P450, glycosyltransferase, glutathione transferase, oxidoreductase), and glucose metabolism conferred metribuzin tolerance in wheat. The validation of DEGs related to photosynthesis (*Lhc a/b*-binding proteins and PSII stability factor HCF136) and metabolic enzymes (cytochrome P450, peroxidase) using RT-qPCR confirmed their responsiveness to metribuzin. Over-expression of transcription factors MYB, AP2-EREBP, ABI3VP1, bHLH, and NAC played a significant roles in regulating photosynthetic and ROS scavenging activities during metribuzin stress. Transcripts with significant enrichments (q-value < 0.05), related to photosynthesis and metabolic detoxification revealed 114 EST-SSRs which may be used as bio-markers.

# Conclusions

The integrative analyses of the data suggests that high amount of sugars, modulation of ROS homeostasis and enhanced photosynthetic activity play a significant role in regulating metribuzin tolerance in wheat. Our data identified master regulators controlling metribuzin tolerance that provide promising avenues for wheat industry.


## Background

Wheat (*Triticum aestivum* L.) is a major global cereal crop in terms of production and area (FAO 2018) and is a staple food for 40% of the global population due to its wide adaptability and easy harvestability [1]. Wheat grows well between the latitudes of 30° and 60° N and 27° and 40° S [2]. The Australian Wheat Promotion Program (2011) proved an important milestone for systematic wheat research and real breakthroughs in productivity but many constraints remain related to dryland farming yields.

Weed infestation is a global problem, more so in Mediterranean-type climatic regions where wheat and weeds actively grow throughout the cropping season. More than 60% of the 20 million ha of arable lands in Australia has a typical Mediterranean-type climate that is characterised by cool, wet winters and hot dry summers [3, 4]. High weed pressure affects tillering in wheat and thereby reduce grain yield. There are instances where weed infestations have reduced wheat yields up to 50% [5]. Weed infestation is estimated to cost $1.3 billion, equivalent to around 20% of the gross value of the Australian wheat crop.

Metribuzin ($C_8H_{14}N_4OS$), a triazine herbicide (group C), is a broad-spectrum herbicide, registered for controlling a range of monocot (grass) and dicot (broad-leafed) weeds, including the most problematic annual ryegrass. Metribuzin is widely used in dryland farming systems in Australia and elsewhere. Pre-emergent application controls weeds during the early stages of growth, between radicle emergence from the seed and seedling leaf emergence through the soil. In particular, pre-emergent application of metribuzin reduced barley and brome grass by over 80% with good wheat yields in Western Australia [6]. Also, the residual activity of metribuzin controls the first few flushes of germinating weeds when the crop is too small to compete and protects the crop from early weed competition. However, the narrow safety margin of metribuzin and lack of selectivity in wheat results in yield losses, limiting its wider use. Apart from its weed control efficacy, tolerance of wheat crops to this herbicide is equally important for maximum crop production.

Herbicide tolerance is an important agronomic trait that allows effective weed management in dryland farming. It is increasingly difficult to discover a new herbicide with a novel mode of action. Expanding the utility of existing broad-spectrum herbicides with a good

environmental profile through genetically enhanced herbicide tolerance is a useful strategy for effective weed management. There is unprecedented scope for developing metribuzin-tolerant wheat cultivars through molecular breeding due to the wide genetic variability for metribuzin tolerance in wheat [7]. Key genes, mechanisms and functional markers involved in herbicide tolerance can be explored using transcriptome analyses for marker-assisted selection (MAS) to develop herbicide-tolerant crops.

The present study aimed to identify (1) the most contrasting genotypes to metribuzin tolerance by assessing the dose-response relationships of nine potential genotypes in a detailed metribuzin dose-response experiment and confirming these genotypes in field conditions, (2) key genes, pathways, and mechanism associated with metribuzin tolerance in the most-tolerant and most-susceptible wheat genotypes using transcriptomic approach (Illumina NovaSeq 6000 platform), and (3) EST-SSR markers for MAS and breeding.

## Results

# Comprehensive screening to identify the most-tolerant and most-susceptible genotypes

The dose-response parameters ($ED_{50}$, $LD_{50}$ and $GR_{50}$) differed significantly in the tolerant and susceptible genotypes (Table 1). Chuan Mai 25 consistently had the highest values across $ED_{50}$, $LD_{50}$ and $GR_{50}$ and highest fold tolerance (R:S ratio) while Ritchie consistently had the lowest values, amongst the nine genotypes (Table 1). Chuan Mai 25 (CM) survived 1717 g a.i. $ha^{-1}$ metribuzin dose whereas Ritchie (R) did not survive the field-recommended rates of 200 g a.i. $ha^{-1}$. The field data confirmed these findings (Fig. 1). Chuan Mai 25 had the lowest senescence and highest survival rate, whereas, Ritchie had the highest senescence and lowest survival rate among all genotypes (Additional file 1: Table S1). This confirms that Chuan Mai 25 and Ritchie are the most-tolerant and most-susceptible genotypes, respectively.

Table 1
Dose-response parameters- $ED_{50}$, $LD_{50}$, and $GR_{50}$ with 95% confidence intervals in parentheses for genotypes

| Genotype | $ED_{50}$[a] (g ai $ha^{-1}$) | 95% CI[b] | $ED_{50}$ R:S ratio[c] | $LD_{50}$ (g ai $ha^{-1}$) | 95% CI[b] | $LD_{50}$ R:S ratio[c] | $GR_{50}$ (g ai $ha^{-1}$) | 95% CI[b] | $GR_{50}$ R:S ratio[c] |
|---|---|---|---|---|---|---|---|---|---|
| Chuan Mai 25 (CM) (T) | 1233 (155) | 925–1540 | 2.8 | 1717 (416) | 893–2541 | 3.6 | 735 (225) | 289–1180 | 2.5 |
| Fundulea 490 (F) (T) | 660 (133) | 495–925 | 1.5 | 1015 (300) | 421–1611 | 2.1 | 453 (72) | 209–496 | 1.2 |
| Eagle Rock (ER) (T) | 891 (123) | 630–1152 | 2.0 | 1596 (229) | 1142–2049 | 3.3 | 613 (68) | 477–749 | 2.1 |
| Kite (K) (T) | 718 (44) | 630–805 | 1.7 | 920 (151) | 620–1220 | 1.9 | 671 (215) | 245–1097 | 2.3 |
| Blade (B) (T) | 1045 (230) | 590–1499 | 2.4 | 1546 (565) | 428–2110 | 3.2 | 659 (242) | 180–1138 | 2.3 |
| W 167 (W) (T) | 699 (113) | 476–921 | 1.6 | 891 (168) | 558–1123 | 1.8 | 683 (249) | 190–1176 | 2.3 |
| Ritchie (R) (S) | 434 (49) | 337–532 | NA | 472 (35) | 401–543 | NA | 286 (79) | 128–444 | NA |
| Spear (S) (S) | 696 (95) | 505–886 | 1.6 | 764 (102) | 560–768 | 1.6 | 307 (32) | 243–372 | 1.0 |
| Dagger (D) (S) | 448 (34) | 380–517 | 1.0 | 480 (32) | 416–545 | 1.0 | 323 (22) | 278–367 | 1.1 |

[a]Standard deviation shown in parenthesis

[b]95% confidence intervals of differential dose

[c]R:S ratios calculated as ratio of $ED_{50}$, $LD_{50}$ and $GR_{50}$ values of resistant and most susceptible (Ritchie) genotypes

$ED_{50}$, metribuzin rate resulting in 50% response in senescence

$LD_{50}$, metribuzin rate resulting in 50% mortality

$GR_{50}$, metribuzin rate resulting in 50% reduction in biomass

Abbreviations: *NA*, not applicable

# Transcriptome Assembly And Novel Genes

The Illumina NovaSeq 6000 platform, generated about 12.38 Gb average bases per sample and 82.54 million clean reads (Table 2). The average mapping ratio of clean reads with the reference genome and gene was 89.6% and 68.4%, respectively. A total of 134,274 novel transcripts were identified, of which 35,420 had a previously unknown splicing event for known genes/novel isoform, 27,699 were novel coding transcripts, and 71,155 were long noncoding RNA. The complete reference transcriptome was obtained by merging the novel coding transcripts with reference transcripts. A summary of the average total genes expressed in three replicates in the control and two treatments, 24 h and 60 h HE are presented in Table 3. After complete transcriptome assembly, an average total of 77,443 genes was identified, of which 59,915 were known genes and 17,528 were novel genes. These genes were compared with the NCBI non-redundant protein for functional annotation.

Table 2
Wheat transcriptome dataset from two extreme genotypes—tolerant (Chuan Mai 25) and susceptible (Ritchie) — in the control and two treatments (24 h and 60 h of herbicide exposure) and a summary of genome mapping

| Genotype | Type | Class | Total raw reads (Mb) | Total clean reads (Mb) | Total clean bases (Gb) | Total mapping ratio (%) | Uniquely mapping ratio (%) |
|---|---|---|---|---|---|---|---|
| Chuan Mai 25 | Tolerant | Control | 90.09 | 82.02 | 12.30 | 88.14 | 68.13 |
| Chuan Mai 25 | Tolerant | Exposed-24 h | 90.09 | 82.60 | 12.39 | 88.87 | 67.05 |
| Chuan Mai 25 | Tolerant | Exposed-60 h | 91.01 | 82.81 | 12.42 | 90.63 | 72.08 |
| Ritchie | Susceptible | Control | 90.47 | 82.34 | 12.35 | 88.36 | 67.12 |
| Ritchie | Susceptible | Exposed-24 h | 91.48 | 82.75 | 12.41 | 91.58 | 72.11 |
| Ritchie | Susceptible | Exposed-60 h | 90.09 | 82.75 | 12.41 | 90.39 | 72.78 |

Total raw reads: reads t before filtering, Unit: Mb; Total clean reads: reads after filtering, Unit: Mb; Total clean bases: total base amount after filtering, Unit: Gb; Total mapping ratio: percentage of mapped reads; Uniquely mapping ratio: percentage of reads that map to only one location of reference

Table 3
Gene statistics used for differentially expressed gene analyses

| Genotype | Type | Class | Total gene number | Known gene number | Novel gene number |
|---|---|---|---|---|---|
| Chuan Mai 25 | Tolerant | Control | 76,070 | 59,456 | 16,614 |
| Chuan Mai 25 | Tolerant | Exposed- 24 h | 76,402 | 59,189 | 17,212 |
| Chuan Mai 25 | Tolerant | Exposed- 60 h | 77,069 | 59,167 | 17,902 |
| Ritchie | Susceptible | Control | 78,567 | 61,397 | 17,170 |
| Ritchie | Susceptible | Exposed- 24 h | 77,578 | 59,837 | 17,741 |
| Ritchie | Susceptible | Exposed- 60 h | 78,975 | 60,443 | 18,532 |

Total gene number: total number of all genes, Known gene number: number of known genes; Novel gene number: number of novel genes

# Identification Of Degs

Gene expression comparisons between Chuan Mai 25 and Ritchie in the control and two treatments (24 h and 60 h HE) revealed commonly and differentially expressed genes (HT-C-vs-HS-C, HT-24 h-vs-HS-24 h and HT-60 h-vs-HS-60 h) (Fig. 2). Most of the DEGs in the inter-groups are related to metribuzin tolerance; the distribution trends of differentially and non-differentially expressed genes, with up-regulated and down-regulated gene numbers in the control and treatments are presented in volcano plots (Additional file 2: Figure S1). The comparison revealed the sum total of commonly and differentially expressed genes: 24,108 in the control (Fig. 2, Additional file 1: Table S2), 24,783 at 24 h HE (Fig. 2, Additional file 1: Table S3) and 23,664 at 60 h HE (Fig. 2, Additional file 1: Table S4). A comparison of HT-24 h-vs-HS-24 h and HT-60 h-vs-HS-60 h revealed a total of 7,736 and 7,460 unique DEGs (Fig. 2), respectively, related to herbicide tolerance in wheat. These DEGs were integrated to investigate the significantly enriched genes and pathways involved in the herbicide tolerance mechanism.

# Transcription Factors And Pathway Analysis Of Degs

A total of 59 transcription factors (TFs) associated with 7,227 DEGs from complete transcriptome were identified (Additional file 2: Figure S2, Additional file 1: Table S5). TFs belonging to MYB (852), MYB-related (701), AP2-EREBP (584), ABI3VP1 (546), bHLH (484), NAC (464), FAR1 (408), mTERF (340), WRKY (300) and MADS (287) families were over-expressed in the metribuzin treatments.

The KEGG enrichment analysis helped us to further understand the biological functions of DEGs. Abundant carbon metabolism, enzyme catalytic activity, binding, transporter and detoxification related GO terms were significantly enriched in biological and molecular function.

Scatterplots showed the top 20 significantly enriched pathways, with 24 h and 60 h HE the most significant (Fig. 3). At 24 h HE (Fig. 3a), significant enrichments occurred for carbon metabolism, fructose and mannose metabolism, homologous recombination, biosynthesis of amino acids, plant-pathogen interaction (R genes), pyrimidine metabolism, galactose metabolism and amino sugar and nucleotide sugar metabolism. The genes regulated around these pathways were early genes generated in response to metribuzin stress. Increased exposure to metribuzin, 60 h HE, caused over-expression of photosynthetic enzymes, ROS scavengers, and phytohormones (glutathione and ascorbic acid) (Fig. 3b).

# Hub Genes Related To Metribuzin Tolerance In Wheat

A total of 107 photosynthesis-related genes were differentially regulated (logFC ≥ 5.0, q-value < 0.05) under metribuzin stress, including genes related to PSI, PSII, light harvesting chlorophyll protein complex (*Lhc)* a/b-binding proteins, PSII stability factor HCF136, PSII oxygen-evolving complex (Additional file 1: Table S6). There is an active participation of *Lhc* a/b-binding proteins in response to metribuzin stress (Fig. 4). *Lhc* a-binding protein and *Lhc* b-binding protein is embedded in thylakoid membrane of PSI and PSII in chloroplast, respectively, which primarily collect and transfers light energy to photosynthetic reaction centres. In this study, most of the *Lhcs'* were down-regulated in susceptible Ritchie but up-regulated in tolerant Chuan Mai 25 under metribuzin stress with 60 h HE. The over-expression of *Lhca1*, *Lhca4*, *Lhcb1-6* in the tolerant Chuan Mai 25 conferred metribuzin tolerance. Enzymatic and non-enzymatic components were synthesised in response to metribuzin stress. The enzymatic components comprise several antioxidant enzymes (Additional file 1: Table S7) involved in alleviating oxidative stress.

# New EST-SSRs for marker-assisted selection

A total of 114 potential EST-SSRs were identified from a total of 660 transcripts containing both novel and known genes. Of the 114 EST-SSRs, 21 were compound microsatellites (Additional file 1: Table S8). The most abundant type was repeated tri-nucleotide (72, 53.3%), followed by di- (56, 41.4%), and tetra- (7, 5.1%). In di-nucleotide repeats, TG (25%) was the most abundant motif (%), followed by GT (14.2%) and TC (14.2%). In tri-nucleotide repeats, CGC (13.8%) was the most abundant motif, followed by GAG (12.5%), CCT (11.1%), and GCC (11.1%). In tetra-nucleotide repeats, GTGC (28.5%) and TGTT (28.5%) were the most abundant motifs. The AGG/CCT motifs had the highest repeat type, followed by AC/GT, AG/CT, and CCG/CGG (Additional file 2: Figure S3).

# Validation of differential expressed genes by RT-qPCR

The fold-changes logFC of gene expression obtained from RNA-seq analysis and RT-qPCR largely corresponded (Table 4) and correlated ($r$ = 0.84) with each other. The two genotypes, Chuan Mai 25 (tolerant) and Ritchie (susceptible), used in transcriptome sequencing responded differently to metribuzin. The RT-qPCR confirmed the involvement of genes related to photosynthesis and metabolic detoxification in metribuzin tolerance. For example, the DEG TraesCS5D01G323800 and TraesCS1D01G096400 involved in metabolic detoxification of herbicide had 3.8 fold increase in expression of cytochrome P450 and peroxidase, respectively, in Chuan Mai 25 than Ritchie. The DEG TraesCS7B01G486500 had 3.1 fold increase in expression of PSII stability/assembly factor HCF136 in Chuan Mai 25 than Ritchie. The DEG TraesCS7D01G276300 expressing *Lhc* a/b-binding proteins in chloroplast had 3.7 fold increased expression in Chuan Mai 25 than Ritchie (Table 4).

Table 4
Gene expression fold-change (FC) measured by RT-qPCR and transcriptome approach

| GENE/Oligo Name | Description | Forward | Reverse | logFC | logFC using qPCR | SE |
|---|---|---|---|---|---|---|
| TraesCS7D01G276300 | chlorophyll a-b binding protein of LHCII type 1 | TTTCCTGGCTGGATTTGTTC | AGTTTTCCCTGTCCCGTTCT | 17.3 | 3.7 | 0.3 |
| TraesCS7B01G471600 | ATP-dependent zinc metalloprotease FTSH 1, chloroplastic | CGCGTGGACTACTACGACTG | GTTGAAGGTGTTCAGCAGCA | 16.3 | 3.6 | 0.1 |
| TraesCS5D01G238300 | chlorophyll a-b binding protein 1B-20, chloroplastic | ATCGCATCAAAAGCCTCATC | CTGCTCAGGTCGTCTTCCTC | 15.7 | 3.8 | 0.8 |
| TraesCS7D01G016800 | ferredoxin-NADP reductase, leaf isozyme, chloroplastic-like | GGAGATCCTGTCGAACAAGC | TCTCCTGCACATCACTTTGC | 14.8 | 2.8 | 0.6 |
| TraesCS1D01G096400 | peroxidase | GCTACCGCTCAAAGGATGAG | AGCACAAACCCTTGGTTGTC | 14.5 | 3.8 | 0.3 |
| TraesCS5B01G275600 | sarcosine oxidase | GATCGTCGACCCACTCTACC | ACCCTTACCAGTGACGATGG | 14.4 | 3.5 | 1.2 |
| TraesCS5D01G530800 | thiol methyltransferase 2 | CCTGTTGCCAAGATTTCCAT | CCGGTTGTCACATTGTCTTG | 14.2 | 3.7 | 0.3 |
| TraesCS7B01G486500 | photosystem II stability/assembly factor HCF136 | GCCAGTAGGCAAAGAGATGC | TAGTCGACCCGGAAGTTGTC | 12.9 | 3.6 | 0.1 |
| TraesCS5D01G323800 | cytochrome P450 71A1 | CGATGCAATGTGCTAGAGGA | TGGCAAAGTCGTGATAGCAG | 12.3 | 3.8 | 0.2 |
| TraesCS7B01G441100 | cytochrome P450 72A14 | TCCCGTCCCAAAAGTAGATG | CTCCATCATCGCCTGTTTCT | 12.2 | 3.7 | 0.1 |
| TraesCS5D01G195000 | arginine N-methyltransferase | AGCCGTTCCATCTCATCTTC | TCGTGCACTGTCGTGTTGTA | 10.9 | 1.0 | 1.3 |
| TraesCS2D01G065200 | ribulose bisphosphate carboxylase small chain PW9, chloroplastic | ACCTGCCGACTTGAGAAAGA | CGTACCAGGAGACGAGCTTC | 10.9 | 1.6 | 0.2 |
| TraesCS5D01G373700 | wall-associated receptor kinase 2 | CACCCTCGAGAACAAGGAGA | ATGGTCTGGATGATGGTGGT | 9.9 | 0.2 | 0.1 |
| TraesCSU01G099100 | expansin | GAAGATGTGTCCAGCAAGCA | CTCAAGGGACCGACGAATTA | 9.7 | 3.1 | 0.3 |
| TraesCS7B01G366200 | nudix hydrolase 14, chloroplastic | AGCAGCAGACATCGCTTGT | GTCGATTGCCTTCTTCCTGA | 8.9 | 2.2 | 0.5 |
| TraesCS7D01G465500 | glyceraldehyde-3-phosphate dehydrogenase GAPCP2, chloroplastic | GGGCTCTGGTGCATACAAAT | TCAAACTGGGCTCTCGTTCT | 7.7 | 0.2 | 0.0 |
| TraesCS7D01G065100 | putative disease resistance protein RGA1 isoform X1 | CCTGCTGTTGCTGTGTTGAT | CAGTGGCAGCAAGATTGGTA | 6.0 | 3.4 | 0.0 |

logFC indicated gene expression level from transcriptome data; logFC using qPCR indicated gene expression level obtained from qPCR.

SE, Standard error

| GENE/Oligo Name | Description | Forward | Reverse | logFC | logFC using qPCR | SE |
|---|---|---|---|---|---|---|
| TraesCS7D01G554000 | E3 ubiquitin-protein ligase ATL44 | GCGTTCTCCTAATGGAGCTG | TGACCTCCTTCCATCCTGAC | 4.9 | 1.7 | 0.4 |
| TraesCS5D01G284500 | Leaf rust 10 disease-resistance locus receptor-like protein kinase | CAAGGAGAAGGAACGACGAC | TAGCAGATGAGGGTGTGCAG | 3.8 | 0.5 | 0.5 |
| TraesCSU01G194100 | Disease resistance protein RPP13 | AGCGCTGGATTCTTCCATAG | AAGCTCCTGAGCTGACCATC | 0 | 0.4 | 0.1 |
| logFC indicated gene expression level from transcriptome data; logFC using qPCR indicated gene expression level obtained from qPCR. | | | | | | |
| SE, Standard error | | | | | | |

## Discussion

We focused on unravelling gene networks, mechanisms and pathways associated with metribuzin tolerance in hexaploid wheat using a unique top-to-bottom three tiered strategy. In the first tier, metribuzin effects were investigated in 946 wheat germplasms (Australian winter wheat collection) from different regions of the world [7]. Our metribuzin tolerance screening identified promising contrasting genotypes. Identification of the most contrasting genotypes is a pre-requisite for better resolution and deeper insight into genes and mechanisms involved in herbicide tolerance. Therefore, in the second tier, a detailed dose-response experiment and field screening were conducted using potential contrasting genotypes to identify the most contrasting genotypes. Chuan Mai 25 and Ritchie were the most contrasting genotypes for metribuzin tolerance when compared with the present known sources. Discovery of the most contrasting genotypes lays a strong foundation for genetic and genomic studies to assist in the development of herbicide-tolerant cultivars with a wide safety margin (Fig. 5). The third tier focused on transcriptome sequencing of Chuan Mai 25 and Ritchie using the Illumina NovaSeq6000 platform. The DEGs identified gene networks, pathways/metabolic enzymes and mechanism(s) contributing to metribuzin tolerance in wheat.

# Mechanism(s) for metribuzin tolerance in wheat

Metribuzin stress limits $CO_2$ fixation and over-reduction of the electron transport chain resulting in ROS [8]. Herbicides generate an abiotic stress that produces ROS, such as $O_2{\cdot}^-$, $H_2O_2$, $^1O_2$, $OH\cdot$, which are extremely toxic and trigger membrane lipid peroxidation and rapid destruction of cellular constituents, resulting in oxidative stress and cell injury or death [9]. Metribuzin is a potent PSII inhibitor. It binds the target site D1 protein in PSII and inhibits electron flow between the primary electron acceptor and plastoquinone. This leads to selective and specific cleavage of the D1 protein. The D1 protein turnover cause the breakdown of PSII, reducing photosynthetic electron transport chain, which produce superoxide radicals and singlet oxygen in the chloroplasts [10-12]. This limits the generation of the energy currencies of cells, ATP and NADPH, inhibiting $CO_2$ fixation in the Calvin cycle.

The present study suggests that metribuzin tolerance in wheat is metabolism-based (Fig. 6). Two major metabolic pathways—glycolysis and pentose phosphate pathway—are over-regulated in response to early metribuzin stress in tolerant wheat. The co-ordinated interplay between these metabolic pathways increases—the influx of energy (ATP), reducing powers [reduced nicotinamide adenine dinucleotide (NADH), NADPH and flavin adenine dinucleotide ($FADH_2$)], and intermediates for biosynthetic and metabolic detoxification processes [13, 14] (Additional file 1: Table S7) are essential for supporting the antioxidant system and preventing oxidative damage to DNA, proteins and lipids [15].

Early genes regulated in response to metribuzin stress (24 h HE) (Fig. 6) belong to carbon metabolism, fructose and mannose metabolism, homologous recombination, amino acid biosynthesis, pyrimidine metabolism, galactose metabolism and amino sugar and nucleotide sugar metabolism. Metabolites such as fructose and mannose are synthesised to protect membranes and proteins from oxidative stress by ROS. Genes involved in homologous recombination are significantly enriched to repair harmful breaks in DNA and restore the essential molecular function in cells [16, 17]. Galactose is involved in glucose synthesis, and pyrimidines serves the role of ATP for glucose synthesis (Zrenner *et al.*, 2006)[18], promoting nutrient remobilisation and preventing senescence.

Increased exposure to metribuzin (60 h) caused over-expression of photosynthetic and metabolic enzymes, antenna proteins (*Lhc* a/b-binding proteins), PSII stability/assembly factor HCF136, and glutathione/ascorbic acid (Fig. 6). Photosynthetic enzymes and antenna proteins are involved in carbon fixation and glucose synthesis catalysed by Rubisco (Additional file 1: Table S6). Glutathione metabolism removes free radicals and prevents oxidative damage to DNA, proteins and lipids. Ascorbic acid (antioxidant) functions as a cofactor for enzymes in photosynthesis, and the synthesis of plant hormones [19] and affects gene expression and transcription, cell division, and growth [20].

## Enzymatic and non-enzymatic components for ROS detoxification

The DEG analysis suggested that metribuzin tolerance is wheat is metabolism-based involving over-expression of several ROS-scavenging enzymes such as superoxide dismutase, catalase, glutathione S-transferase (GSTs), glutathione peroxidase, cytochrome P450 (CYPs), cytochrome reductase, cytochrome peroxidase, oxidoreductase, ABC transporters, glycosyltransferase (GT), UDP-galactosyltransferase and ubiquitin transferase to prevent oxidative stress during herbicide stress in the tolerant wheat genotype, Chuan Mai 25. Some of the herbicide is detoxified before it reaches target site. CYPs add a reactive group such as hydroxyl, carboxyl, or an amino group through oxidation to herbicide molecule, making it a polar molecule (phase I detoxification) and transferases (phase II detoxification enzymes) conjugates the addition of water-soluble group to the reactive site of polar molecule. The identified gene superfamilies or domains are essentially xenobiotic detoxifying enzymes involved in vacuolar sequestration of conjugated herbicide metabolites. The non-enzymatic components/phytohormones such as ascorbic acid and glutathione (GSH) have ROS scavenging function and plays a protective role during metribuzin stress. GSH function with GSTs to detoxify herbicides by tagging electrophilic compounds for removal during oxidative stress [21, 22].

Overexpression of ROS-responsive regulatory genes (Additional file 1: Table S6, S7), which regulate a large set of genes involved in acclimation mechanisms, is a powerful strategy for enhancing herbicide tolerance in wheat. The ability of wheat genotypes to metabolize herbicides are largely dependent on the genetic expression of these enzymes. Difference in metribuzin tolerance expression is a result of genetic polymorphisms resulting in an altered expression. This is confirmed by SNP discovery in metribuzin-tolerant and –susceptible wheat groups using 90K iSelect SNP genotyping assay. The polymorphic SNP loci between the two groups detected genes on chromosomes (2A, 2D, 3B, 4A, 4B, 7A, 7B, 7D) encoding metabolic detoxification enzymes (cytochrome P450, glutathione S-transferase, glycosyltransferase, ATP-binding cassette transporters and glutathione peroxidase) [23]. We have mapped QTLs for metribuzin tolerance in wheat. The genes underlying the QTL support range on chromosomes-1AS (oxidoreductase), 2DS (glycosyltransferase), 4AL (transferase activity) are involved in metabolic detoxification. The integration of present transcriptomic analyses, previous metribuzin-tolerant QTL mapping [6], and SNP discovery using 90K iSelect SNP genotyping assay in metribuzin-tolerant and -susceptible wheat genotypes [7] suggests that enzymatic components play a significant role in modulating ROS homeostasis and the acclimation response of wheat to metribuzin tolerance.

## Over-Expression of *Lhc* a/b-binding proteins and PSII stability/assembly factor HCF136 confers metribuzin tolerance in wheat

PSII functions as a water-plastoquinone oxidoreductase in oxygenic photosynthesis. The redox components, required for PSII function are localised on the heterodimer of the Dl and D2 proteins of the PSII reaction centre (Fig. 4). *Lhc* a/b-binding proteins are typically complexed with chlorophyll and xanthophylls and serve as the antenna complex, which regulate the distribution of excitation energy between PSII and PSI [24]. Regulation of *Lhc* a/b-binding proteins is an important mechanism in plants to modulate chloroplast functions [25, 26]. This study suggests that over-expression of *Lhc* a/b binding proteins in metribuzin tolerant wheat (Chuan Mai 25), promotes carbon fixation and modulates ROS homeostasis during metribuzin stress.

HCF136—the thylakoid-embedded large pigment-protein complexes of the photosynthetic electron transfer chain—is involved in the assembly of PSII reaction centre complexes, *de novo* synthesis of the D1 protein and the selective replacement of damaged D1 protein during PSII repair [27]. Lower expression of HCF136 in susceptible Ritchie during metribuzin stress resulted in the accumulation of damaged PSII proteins, which increased oxidative stress. Photosynthesis cease when degradation and PSII repair do not balance under herbicide stress. This implies that in susceptible wheat, a reduction in fundamental processes such as photosynthesis produce oxidative stress in chloroplast, which extends beyond PSII to cause a down-regulation of total carbon gain and imbalance between the rate of photo-damage to PSII and the rate of the repair of damaged PSII, reducing plant yield in susceptible genotypes. 90K iSelect SNP genotyping assay in our previous investigation detected polymorphism between tolerant and susceptible wheat genotypes in the gene encoding PSII

assembly factor involved in PSII repair [23]. This suggests that metribuzin-tolerant wheat genotypes have inherently high photosynthetic efficiency.

# Transcription factors

Biotic and abiotic stresses trigger a wide range of plant responses, from the alteration of gene expression and cellular metabolism to changes in plant growth and development. The TFs play critical roles in regulating stress responses in plants. The present study suggests that TFs belonging to the MYB, AP2-EREBP, ABI3VP1, bHLH, NAC, FAR1, mTERF, WRKY families are over-expressed to enrich ROS scavenging activity and photosynthetic genes during metribuzin stress in tolerant wheat. The MYB and NAC genes are the largest families of plant-specific TFs that play important roles in the regulation of the transcriptional reprogramming of plant stress responses. Genetic and molecular studies using knockout/knockdown mutants and overexpression in model plants and crop plants have demonstrated that TFs belonging to the MYB, NAC [28-30], AP2/EREBP [31], WRKY [32, 33], and bHLH families play important roles in plant responses to abiotic and biotic stresses [34].

# Herbicide-tolerant wheats

The EST-based SSR markers identified in significantly enriched genes relating to photosynthetic and metabolic detoxification enzymes with present-absent variation (PAV), with significant differential expression will be a great resource for metribuzin tolerance breeding. The PAV is a sequence in one genome, but entirely missing in another genome. This is an important source of genetic diversity in plants [35, 36]. We propose the use of functional specific markers for a desired traits which reduces genotype-phenotype gaps in crop plants to maximize genetic gains in breeding. High-throughput identification of PAV on a whole-genome level has become possible with the advent of next-generation sequencing (NGS) technologies, at affordable prices [37]. There is a rapidly rising trends in the application of genome editing based crop improvement using CRISPR/Cas genome engineering system [38, 39]. The improved understanding of genetic and genomic knowledge of herbicide tolerance will open up the utilities for inducing multiple cleavage events, controlling gene expression, and site specific transgene insertion.

In conclusion, the use of improved metribuzin-tolerant wheats will help farmers to (1) minimise the early cohorts of problematic weeds, removing early wheat and weed competition and increasing wheat productivity, and (2) promote crop rotations with other herbicide-tolerant crops, such as narrow-leafed lupin (*Lupinus angustifolius* L.) and canola (*Brassica napus* L.) to assist in sustainable farming systems.

## Methods

# Herbicide

Metribuzin ($C_8H_{14}N_4OS$), a triazinone herbicide was purchased from Syngenta Crop Protection. Metribuzin binds its target site D1 protein in PSII and inhibits electron flow between the primary electron acceptor to plastoquinone, arresting photosynthesis. The metribuzin dose of 400 g a.i. $ha^{-1}$ was used to create stimulus/stress in tolerant and susceptible genotype.

# Plant material

Contrasting wheat genotypes, six herbicide-tolerant (HT) and three herbicide-susceptible (HS) (Table 1) identified amongst 946 wheat genotypes from six continents (Australian winter cereals collection) [7] and Western Australian local cultivars [40] —were selected for the detailed dose-response experiment and field screening. The two most-contrasting genotypes, Chuan Mai 25 (HT) (origin: China; type: spring) and Ritchie (HS) (origin: England; type: spring) were used for transcriptome sequencing. Chuan Mai 25 is an advanced cultivar, with a very good disease resistance, which was released in 1995.

# Detailed dose-response and field screening

A detailed dose-response experiment with pre-emergent application was conducted in glasshouse to determine the most contrasting genotypes and dose-response parameters such as $ED_{50}$ value (rate of application for 50% reduction in visual senescence/chlorosis), $LD_{50}$ value (rate of application to kill 50% of plants) and $GR_{50}$ value (rate of application for 50% growth reduction). Seeds were sown in 10 cm pots and sprayed with eight metribuzin rates (0, 100, 200, 400, 800, 1600, 3200 and 6400 g a.i. $ha^{-1}$) via a twin flat-fan nozzle

perpendicular to the direction of sowing in two passes at 200 kPa in a cabinet spray chamber calibrated to deliver 118 L water $ha^{-1}$. The trial was carried out in 2018 in a UWA glasshouse, Australia. The trial comprised nine rows by three columns for each metribuzin rate. Each genotype × herbicide treatment was replicated three times with seven plants per replicate. Plants were watered every 48 h to ensure that moisture was non-limiting. At 21 days after treatment (DAT), senescence/chlorosis was rated using a scale of 0 (no senescence/phytotoxicity) to 10 (100% senescence/dead). Percentage survival was determined by scoring as 'dead' or 'alive' for all the rates. The above-ground biomass was harvested and expressed as a percentage of the mean untreated control. Dose-response analyses were carried out using R extension package '*drc*'. Senescence was fitted to the three-parameter log-logistic function '*LL*.3*'* where the lower limit is equal to 0 to determine $ER_{50}$. Survival and biomass were fitted to the four-parameter log-logistic function '*LL*.4*'* to determine $LD_{50}$ and $GR_{50}$.

Field screening was conducted to validate the metribuzin effects (data for W167 and Blade not available) during winter 2018 at the Shenton Park Field Station, Perth, Western Australia (coordinates: 31.9480˚S, 115.7955˚E). The R '*agricolae'* package was used to generate a randomised complete block design with three columns by seven rows, each column represented a replicate block. Each plot was 1 $m^2$, with six rows spaced 20 cm apart and each row had approximately 20 plants at 5 cm spacing, with approximately 120 plants per plot. Herbicide rates spanned the estimated $LD_{50}$ confidence range (0, 200, 400 and 800 g a.i. $ha^{-1}$). Each herbicide rate had three randomised replicate plots in three blocks. Metribuzin was sprayed using a hand-held liquid herbicide applicator immediately after sowing. At 21 DAT, senescence and survival rate were recorded as described above. Dot plots for field screening data were generated using the '*ggplot2'* library in R.

# Tissue collection and RNA isolation

The two most-contrasting wheat genotypes, Chuan Mai 25 (HT) and Ritchie (HS) were analysed for transcriptome sequencing. Seeds were surface sterilised in 3% NaClO, for 10 min and washed three times followed by 24 h imbibition in double-distilled water. The seedlings were propagated in 1 L pots containing river sand in a growth chamber at 25°C/15°C (day/night) with a 16 h photoperiod at a light intensity of 800±200 µE $m^{-2}$ $s^{-1}$ and 8 h dark and relative humidity (55%). Twelve days after sowing fully-grown seedling (3–5 leaf stage) in three replicates were uniformly sprayed with metribuzin at 400 g ai $ha^{-1}$ using a twin flat-fan nozzle as described above. Young leaf tissue was harvested aseptically from the control and treatments after 24 h and 60 h herbicide exposure (HE) and frozen immediately in liquid nitrogen and stored at −80°C for RNA isolation. Total RNA was isolated using an RNA plant mini kit (BIOLINE) according to the manufacturer's instructions. RNA quantity and quality were measured with a Bioanalyzer.

# Library preparation and pre-processing of transcriptome datasets

Illumina sequencing was performed using next-generation high-throughput NovaSeq 6000 RNA-Seq platform according to the manufacturer's instructions (Illumina, San Diego, CA). Illumina paired-end reads (2 × 100 bp) were generated using RNA of Chuan Mai 25 (HT) and Ritchie (HS). NovoSeq 6000 sequencing platform generated an average of 12.38 Gb bases per sample. The raw reads were pre-processed before downstream analyses for (1) adaptor contamination, (2) reads with unknown nucleotides comprising more than 5%, (3) low quality reads with ambiguous sequence 'N',, and (4) very short (35 bp) sequences using SOAPnuke software (v1.5.2 available at https://github.com/BGI-flexlab/SOAPnuke). The sequencing data have been submitted to the Sequence Read Archive in National Centre for Biotechnology Information (NCBI); BioProject ID: PRJNA555667, BioSample accession: SAMN12325611.

# Transcriptome assembly and novel transcripts prediction

Processed high-quality clean reads were mapped to the reference genome using HISAT (v2.0.4 available at http://www.ccb.jhu.edu/software/hisat) [41]. Mapping results were viewed using the Integrative Genomics Viewer tool which supports multiple sample comparisons and shows the distribution of reads in exon, intron, UTR and intergenic areas based on the annotation result. After genome mapping, String Tie (v1.0.4 available at http://ccb.jhu.edu/software/stringtie) [42] was used to reconstruct novel transcripts identified using Cuffcompare, a tool of Cufflinks (v2.2.1 available at http://cole-trapnell-lab.github.io/cufflinks) [43] and the coding ability of novel transcripts was predicted by using CPC (v0.9-r2 available at http://cpc.cbi.pku.edu.cn) [44]. The novel coding transcripts were merged with reference transcripts to obtain the complete reference before mapping the clean reads to the reference genome using Bowtie2 [45]. Subsequently, novel genes, SNP and INDELs were detected.

## Gene expression analysis

The gene expression level for each sample was calculated using a RSEM software (v1.2.12 available at http://deweylab.biostat.wisc.edu/RSEM) [46]. The relative transcript abundance in the different treatment groups was obtained using the FPKM method (fragments per kilobase of transcript per million mapped reads) [47]. FPKM = (1000000*C)/(N*L/1000), C represents the amount of fragment mapped to the specific transcripts, N represents the amount of fragment mapped to any transcripts and L represents the base amount of the specific transcripts. Differentially expressed genes (DEGs) are detected based on the poisson distribution of DEGseq [48]. To delineate herbicide resistance mechanism(s) in the wheat transcriptome, DEGs were grouped into three combinations, namely, HT-C-vs-HS-C, HT-24h-vs-HS-24h and HT-60h-vs-HS-60h. TFs were classified based on DEGs. The genes significantly enhanced with cut-off logFC ≥ 5.0 were used to identify the metabolic pathways associated with metribuzin tolerance in wheat

## DEG analyses

DEGs were classified according to official classification based on gene ontology (GO) functional enrichment and pathway functional enrichment using '*phyper',* a function of R. A cut-off value of false discovery rate (FDR) ≤ 0.01 was used to filter the significant enrichment. A *'getorf'* was used to find open reading frame (ORF) of DEGs. ORFs were aligned to *TF* domains (from PlnfDB) using hmmsearch (v3.0 available at http://hmmer.org). To obtain the interaction between DEG encoded proteins, we used DIAMOND (v0.8.31 available at https://github.com/bbuchfink/diamond) [49] to map the DEGs to the STRING database (v10 available at http://string-db.org/) [50]. Cytoscape software was used for network analysis and visualization.

## New EST-SSR markers for metribuzin tolerance in wheat

A universal web-tool, *PolyMorphPredict* (http://webtom.cabgrid.res.in/polypred/) [51] was used to identify SSRs contributing to metribuzin tolerance in wheat. Gene transcripts related to photosynthesis (PSI and PSII), ROS scavengers, phytohormones and metabolic detoxification, with PAV or higher-fold expression (logFC ≥ 5.0, q-value < 0.05) (Additional file 1: Table S6, S7), were used to survey potential SSRs. The mono-, di-, tri-, tetra-, penta-, and hexa-nucleotides were designed with minimum repeat numbers of 10, 6, 5, 5, 5, and 5 for the SSRs, respectively.

## Validation of RNA-seq analysis and DEGs related to photosynthesis/antenna proteins, and metabolic enzymes using RT-qPCR

To confirm the RNA-seq results, 20 DEGs were randomly selected and assessed using RT-qPCR. RT-qPCR primers were designed using Primer 3 software [52, 53]. First-strand cDNA synthesis was done using SensiFAST™ (BIOLINE) as per the manufacturer's protocol. RT-qPCR was conducted on a Real-Time PCR system (7500 Applied Bio systems Foster, CA, USA) using SYBR Green for the detection of PCR products. Each reaction was performed in a final volume of 16 µL, containing 8 µL SYBR Green PCR Master Mix (Applied Biosystems), 250 nM of each primer and 50 ng cDNA template. The thermal cycling conditions were 94˚C for 10 min, followed by 40 cycles of 94˚C for 15 s, 55˚C for 30 s, and 60˚C for 1 min, with fluorescent detection at the end of each cycle. The amplification of a single product per reaction was confirmed by melting curve analysis. The wheat actin 2 gene was used as the housekeeping gene for normalisation of Ct values of each reaction. All reactions were performed in triplicates and $\Delta\Delta C_T$ values were obtained for gene expression fold-change analysis. The sequences of the primers for selected genes used in RT-qPCR analysis are listed in Table 4.

The expression pattern of significantly enriched DEGs under metribuzin treatment (60 h HE), were assessed. We mainly focused on DEGs related to photosynthesis and metabolic enzymes: TraesCS7B01G486500 (PSII stability factor HCF136), TraesCS7D01G276300 (*Lhc* a/b-binding proteins), TraesCS5D01G238300 (*Lhc* a/b-binding proteins), TraesCS5D01G323800 (cytochrome P450), TraesCS7B01G441100 (cytochrome P450) and TraesCS1D01G096400 (peroxidase).

## Abbreviations

ED50: Rate of application for 50% reduction in visual senescence/chlorosis LD50: Rate of application to kill 50% of plants GR50: Rate of application for 50% growth reduction CM: Chuan Mai 25 R: Ritchie ROS: Reactive oxygen species Lhc: Light-harvesting chlorophyll a/b-binding proteins PSII: Photosystem II PSI: Photosystem I EST: Expressed sequence tags SSR: Simple sequence repeats MAS: Marker-assisted selection HE: Herbicide exposure NCBI: National center for biotechnology information DEGs: Differentially expressed genes TFs:

Transcription factors KEGG: Kyoto encyclopedia of genes and genomes qPCR: Real-time polymerase chain reaction logFC: Fold change gene expression ATP: Adenosine triphosphate NADPH: Nicotinamide adenine dinucleotide phosphate GST: Glutathione S transferase CYPs: Cytochrome P450 GT: Glycosyltransferase GSH: Glutathione QTL: Quantitative trait loci PAV: Present-absent variation NGS: Next-generation sequencing

# Declarations

### Ethics approval and consent to participate

Not applicable

### Consent for publication

Not applicable

### Availability of data and materials

The datasets supporting the conclusions of this article are available in the NCBI repository with accessions (BioProject ID: PRJNA555667, BioSample accession: SAMN12325611). The source data underlying supplementary Figures 1–3 and supplementary Tables 1–8 are provided as a Source Data file in this published article.

### Competing interests

The authors declare that they have no competing interests


### Funding

Yitpi Foundation Research Awards (Plant Breeders' Rights Act), South Australia supported the design of the study and covered the expenses of field trial, RNA sequencing, data collection, and data analyses. Roopali acknowledges the Research Training program scholarship from the Australian Government that sponsored her PhD study.


### Authors' contributions

RB, PS, KHMS and GY conceived the project and designed scientific objectives; RB and GY designed methodology; RB conducted experimental design and performed data analysis; RB wrote the draft manuscript; and KHMS, PS and GY revised the paper. All authors discussed the results, read and approved the final manuscript for publication.


### Acknowledgements

We thank BGI, Hong Kong for NGS services. We thank Dr Ifeyinwa Onyemaobi, Dr Xingyi Wang and Dr Hui Liu for technical help.



### Author details

[1]UWA School of Agriculture and Environment, The University of Western Australia, Perth, WA 6009, Australia. [2]The UWA Institute of Agriculture, The University of Western Australia, Perth, WA 6009, Australia.


# References


1. Shiferaw B, Smale M, Braun HJ, Duveiller E, Reynolds M, Muricho G. Crops that feed the world 10. Past successes and future challenges to the role played by wheat in global food security. Food Security. 2013;5(3):291–317.
2. Curtis BC, Rajaram S, Gómez M. Bread wheat: improvement and production: Food and Agriculture Organization of the United Nations (FAO). 2002.
3. Siddique K, Brinsmead R, Knight R, Knights E, Paull J, Rose I. Adaptation of chickpea (*Cicer arietinum* L.) and faba bean (*Vicia faba* L.) to Australia. In: Linking research and marketing opportunities for pulses in the 21st century, Springer; 2000. p. 289–303.
4. Turner NC, Asseng S. Productivity, sustainability, and rainfall-use efficiency in Australian rainfed Mediterranean agricultural systems. Aust J Agric Res. 2005;56(11):1123–36.
5. Kleemann SG, Gill GS. Applications of metribuzin for the control of rigid brome (*Bromus rigidus*) in no-till barley crops of southern Australia. Weed Technol. 2009;22:34–7.

6. Haskins B, MacLennan A. Managing annual ryegrass in cropping systems – pre and post emergent herbicide trial. Barellan: GRDC Update; 2014.
7. Bhoite RN, Si P, Stefanova KT, Siddique KH, Yan G. Identification of new metribuzin-tolerant wheat (*Triticum* spp.) genotypes. Crop Pasture Sci. 2017;68(5):401–8.
8. Mittler R, Vanderauwera S, Gollery M, Van Breusegem F. Reactive oxygen gene network of plants. Trends Plant Sci. 2004;9(10):490–8.
9. Sharma P, Jha AB, Dubey RS, Pessarakli MJ. Reactive oxygen species, oxidative damage, and antioxidative defense mechanism in plants under stressful conditions. J. Botany. 2012:2012, https://doi.org/10.1155/2012/217037.
10. Bechtold U, Murphy DJ, Mullineaux PM. Arabidopsis peptide methionine sulfoxide reductase2 prevents cellular oxidative damage in long nights. The Plant Cell. 2004;16(4):908–19.
11. HongBo S, ZongSuo L, MingAn S, ShiMeng S, ZanMin H. Investigation on dynamic changes of photosynthetic characteristics of 10 wheat (*Triticum aestivum* L.) genotypes during two vegetative-growth stages at water deficits. Colloids Surf B Biointerfaces. 2005;43:221–7.
12. Li J, Jin H. Regulation of brassinosteroid signaling. Trends Plant Sci. 2007;12(1):37–41.
13. Keller MA, Turchyn AV, Ralser M. Non-enzymatic glycolysis and pentose phosphate pathway-like reactions in a plausible Archean ocean. Mol Syst Biol. 2014;10(4):725.
14. Ma HL, Xu XH, Zhao XY, Liu HJ, Chen H. Impacts of drought stress on soluble carbohydrates and respiratory enzymes in fruit body of *Auricularia auricula*. Biotechnol Biotechnological Equipment. 2015;29(1):10–4.
15. De Freitas-Silva L, Rodríguez-Ruiz M, Houmani H, Da Silva LC, Palma JM, Corpas FJ. Glyphosate-induced oxidative stress in *Arabidopsis thaliana* affecting peroxisomal metabolism and triggers activity in the oxidative phase of the pentose phosphate pathway (OxPPP) involved in NADPH generation. J Plant Physiol. 2017;218:196–205.
16. Bray CM, West CE. DNA repair mechanisms in plants: crucial sensors and effectors for the maintenance of genome integrity. New Phytol. 2005;168(3):511–28.
17. Yoshiyama K, Sakaguchi K, Kimura SJ. DNA damage response in plants: conserved and variable response compared to animals. Biology. 2013;2(4):1338–56.
18. Zrenner R, Stitt M, Sonnewald U, Boldt R. Pyrimidine and purine biosynthesis and degradation in plants. Annu Rev Plant Biol. 2006;57:805–36.
19. Gallie DR. L-ascorbic acid: a multifunctional molecule supporting plant growth and development. Scientifica. 2013:2013, https://doi.org/10.1155/2013/795964.
20. Hussain Q, Shi J, Scheben A, Zhan J, Wang X, Liu G, Yan G, King GJ, Edwards D, Wang H. Genetic and signalling pathways of dry fruit size: targets for genome editing-based crop improvement. Plant Biotechnol J. 2020;18(5):1124.
21. Marrs KA, Walbot V. Expression and RNA splicing of the maize glutathione S-transferase Bronze2 gene is regulated by cadmium and other stresses. Plant Physiol. 1997;113(1):93–102.
22. Edwards R, Dixon DP, Walbot VJ. Plant glutathione S-transferases: enzymes with multiple functions in sickness and in health. Trends Plant Sci. 2000;5(5):193–8.
23. Bhoite R, Si P, Liu H, Siddique K, Yan G, Xu L. Inheritance of pre-emergent metribuzin tolerance and putative gene discovery through high-throughput SNP array in wheat (*Triticum aestivum* L.). BMC Plant Biol. 2019;19:457.
24. Jansson S. The light-harvesting chlorophyll ab-binding proteins. Biochimica et Biophysica Acta (BBA)-Bioenergetics. 1994;1184(1):1–19.
25. de Montaigu A, Tóth R, Coupland G. Plant development goes like clockwork. Trends Genet. 2010;26(7):296–306.
26. Pruneda-Paz JL, Kay SA. An expanding universe of circadian networks in higher plants. Trends Plant Sci. 2010;15(5):259–65.
27. Komenda J, Nickelsen J, Tichý M, Prášil O, Eichacker LA, Nixon PJ. The cyanobacterial homologue of HCF136/YCF48 is a component of an early photosystem II assembly complex and is important for both the efficient assembly and repair of photosystem II in Synechocystis sp. PCC 6803. J Biol Chem. 2008;283(33):22390–9.
28. Puranik S, Sahu PP, Srivastava PS, Prasad M. NAC proteins. regulation and role in stress tolerance. Trends Plant Sci. 2012;17(6):369–81.
29. Nuruzzaman M, Sharoni AM, Kikuchi S. Roles of NAC transcription factors in the regulation of biotic and abiotic stress responses in plants. Frontiers Microbiol. 2013;4:248.
30. Shao H, Wang H, Tang X. NAC transcription factors in plant multiple abiotic stress responses: progress and prospects. Frontiers Plant Sci. 2015;6:902.

31. Mizoi J, Shinozaki K, Yamaguchi-Shinozaki K. AP2/ERF family transcription factors in plant abiotic stress responses. Biochimica et Biophysica Acta (BBA)-Gene Regulatory Mechanisms. 2012;1819(2):86–96.
32. Chen L, Song Y, Li S, Zhang L, Zou C, Yu D. The role of WRKY transcription factors in plant abiotic stresses. Biochimica et Biophysica Acta (BBA)-Gene Regulatory Mechanisms. 2012;1819(2):120–8.
33. Rushton DL, Tripathi P, Rabara RC, Lin J, Ringler P, Boken AK, Langum TJ, Smidt L, Boomsma DD, Emme NJ. WRKY transcription factors: key components in abscisic acid signalling. Plant Biotechnol J. 2012;10(1):2–11.
34. Nakashima K, Yamaguchi-Shinozaki K, Shinozaki K. The transcriptional regulatory network in the drought response and its crosstalk in abiotic stress responses including drought, cold, and heat. Frontiers Plant Sci. 2014;5:170.
35. Batley J, Barker G, O'Sullivan H, Edwards KJ, Edwards D. Mining for single nucleotide polymorphisms and insertions/deletions in maize expressed sequence tag data. Plant Physiol. 2003;132(1):84–91.
36. Gao Q, Yue G, Li W, Wang J, Xu J, Yin Y. Recent Progress Using High-throughput Sequencing Technologies in Plant Molecular Breeding F. J Integrative Plant Biol. 2012;54(4):215–27.
37. Tester M, Langridge P. Breeding technologies to increase crop production in a changing world. Sci. 2010;327:818–22.
38. Zhang Z, Hua L, Gupta A, Tricoli D, Edwards KJ, Yang B, Li W. Development of an Agrobacterium-delivered CRISPR/Cas9 system for wheat genome editing. Plant Biotechnol J. 2019;17(8):1623–35.
39. Schaeffer SM, Nakata PA. CRISPR/Cas9-mediated genome editing and gene replacement in plants: transitioning from lab to field. Plant Sci. 2015;240:130–42.
40. Kleemann SG, Gill GS. Differential tolerance in wheat (*Triticum aestivum* L.) genotypes to metribuzin. Crop Pasture Sci. 2007;58(5):452–6.
41. Kim D, Langmead B, Salzberg SL. HISAT: a fast spliced aligner with low memory requirements. Nat Methods. 2015;12(4):357.
42. Pertea M, Pertea GM, Antonescu CM, Chang TC, Mendell JT, Salzberg SL. StringTie enables improved reconstruction of a transcriptome from RNA-seq reads. Nat Biotechnol. 2015;33(3):290.
43. Trapnell C, Roberts A, Goff L, Pertea G, Kim D, Kelley DR, Pimentel H, Salzberg SL, Rinn JL, Pachter LJ. Differential gene and transcript expression analysis of RNA-seq experiments with TopHat and Cufflinks. Nat Protocols. 2012;7(3):562.
44. Kong L, Zhang Y, Ye Z-Q, Liu X-Q, Zhao S-Q, Wei L, Gao GJ. CPC: assess the protein-coding potential of transcripts using sequence features and support vector machine. Nucleic Acids Res. 2007;35:W345-W9.
45. Langmead B, Salzberg SL. Fast gapped-read alignment with Bowtie 2. Nat Methods. 2012;9(4):357.
46. Li B, Dewey CN. RSEM: accurate transcript quantification from RNA-Seq data with or without a reference genome. BMC Bioinfo. 2011;12(1):323.
47. Anders S, Huber W. Differential expression analysis for sequence count data. Genome Biol. 2010;11(10):R106.
48. Wang L, Feng Z, Wang X, Wang X, Zhang X. DEGseq: an R package for identifying differentially expressed genes from RNA-seq data. Bioinformatics. 2009;26(1):136–8.
49. Buchfink B, Xie C, Huson DH. Fast and sensitive protein alignment using DIAMOND. Nat Methods. 2015;12(1):59.
50. Von Mering C, Jensen LJ, Snel B, Hooper SD, Krupp M, Foglierini M, Jouffre N, Huynen MA, Bork P. STRING: known and predicted protein–protein associations, integrated and transferred across organisms. Nucleic Acids Res. 2005;33:D433-D7.
51. Das R, Arora V, Jaiswal S, Iquebal MA, Angadi UB, Fatma S, Singh R, Shil S, Rai A, Kumar D. PolyMorphPredict: A universal web-tool for rapid polymorphic microsatellite marker discovery for whole genome and transcriptome data. Frontiers Plant Sci. 2018;9:1966.
52. Koressaar T, Remm MJ. Enhancements and modifications of primer design program Primer3. Bioinformatics. 2007;23(10):1289–91.
53. Untergasser A, Cutcutache I, Koressaar T, Ye J, Faircloth BC, Remm M, Rozen SG. Primer3—new capabilities and interfaces. Nucleic Acids Res. 2012;40(15):e115.

## Figures

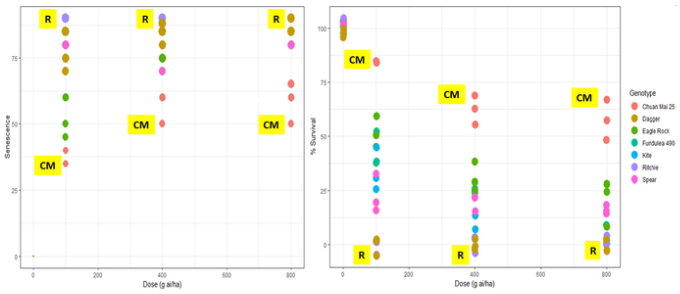


**Figure 1**

Dot plots showing metribuzin response of seven wheat cultivars in a field trial, measured in terms of senescence (left) and % survival (right) at different doses [0 (control), 100, 400 and 800 g a.i. ha−1]. Genotypes are represented by different coloured dots. CM, Chuan Mai 25; R, Ritchie.

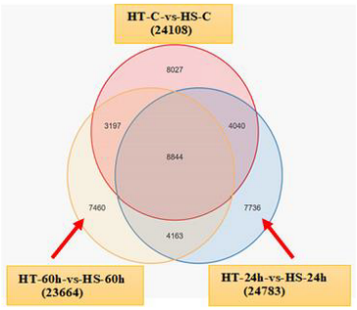


**Figure 2**

Venn diagram showing overlap of differentially expressed genes in metribuzin-tolerant, Chuan Mai 25 and metribuzin-susceptible, Ritchie at 0 h (pink), 24 h (blue) and 60 h (yellow) metribuzin-treatments.

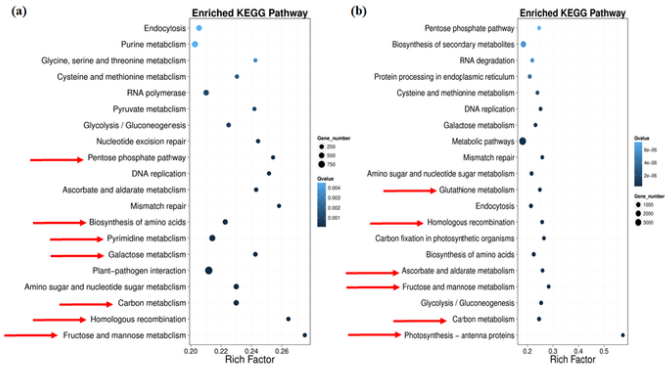


## Figure 3

(a) Scatterplot of enriched KEGG analyses for DEGs at different 24 h and 60 h after metribuzin exposure. The rich factor indicates the ratio of DEG numbers annotated in this pathway group to total gene numbers annotated in this pathway group. The larger the rich factor, the larger the degree of pathway enrichment. Point colour indicates the q-value (high: white, low: blue), lower q-values in darker blue indicate more significant enrichment. Point size indicates DEG number (bigger dots reflect to larger amounts) and (b) most significantly enriched KEGG-DEG (differential expression gene) relationship network. Red arrows are the most significantly enriched pathways.

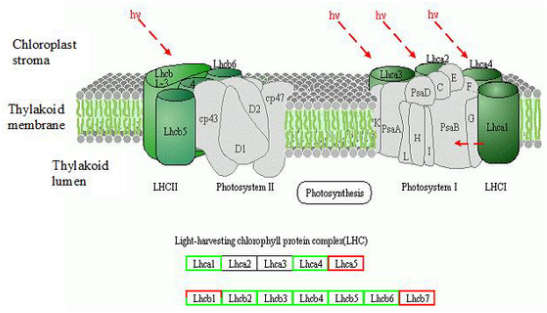


**Figure 4**

Photosynthesis antenna proteins with light harvesting chlorophyll antenna/protein complex (LHII and LHI) on PSII and PSI in Plants (Source: Kanehisa Laboratories). Up-regulated genes in response to metribuzin in tolerant Chuan Mai 25 are marked with green border and down-regulated genes in response to metribuzin in tolerant Chuan Mai 25 are marked with red border and no-change genes are marked with black border.

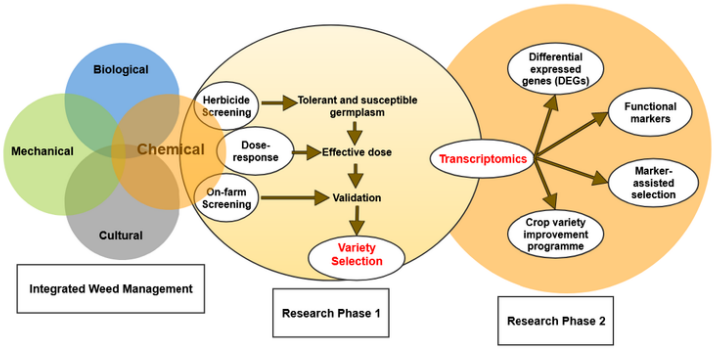


**Figure 5**

Proposed model showing research phases and accelerated pre-breeding strategies to develop herbicide-tolerant cultivars.

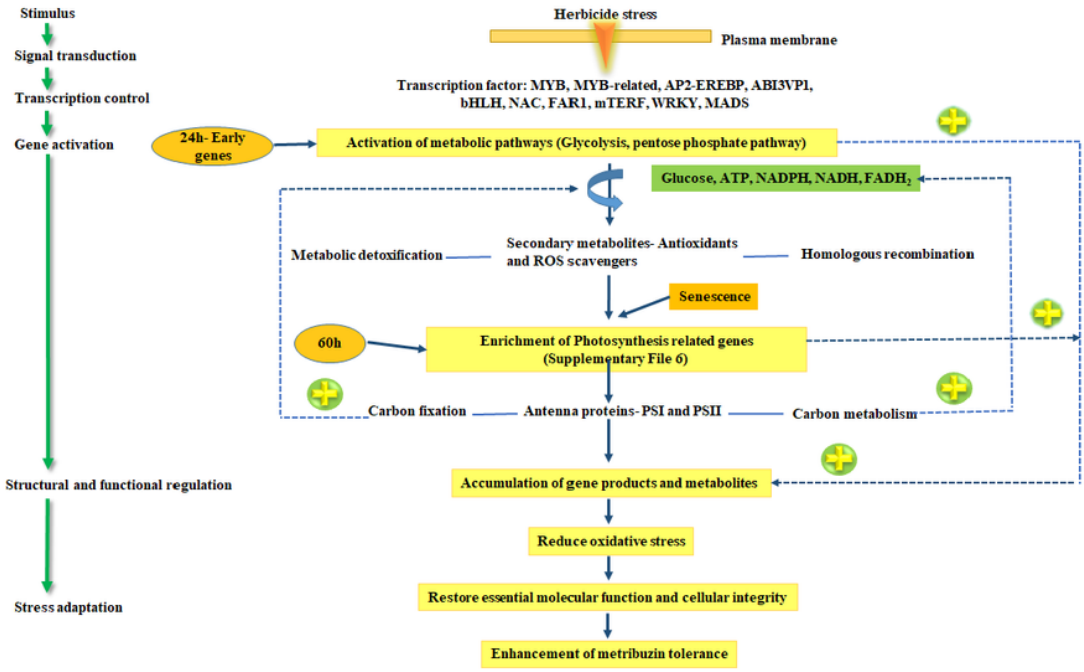


**Figure 6**

Proposed mechanism for signal transduction, transcription regulation and gene activation for metribuzin stress adaptation in tolerant wheat.

## Supplementary Files

This is a list of supplementary files associated with this preprint. Click to download.

- SupplementaryFigures.pdf
- AdditionalFile1TableS8.xlsx
- AdditionalFile1TableS7.xlsx
- AdditionalFile1TableS6.xlsx
- AdditionalFile1TableS5.xlsx
- AdditionalFile1TableS4.xlsx
- AdditionalFile1TableS3.xlsx
- AdditionalFile1TableS2.xlsx
- AdditionalFile1TableS1.xlsx